Flavin-Cytochrome Complexes Transfer Electrons among *Shewanella oneidensis* MR-1 Cells

Yoshihide Tokunou[1,2#], Hiromasa Tongu[3], Akihiro Okamoto[1,2,4], Masanori Toyofuku[1,5], and Nobuhiko Nomura[1,5]

1. Faculty of Life and Environmental Sciences, University of Tsukuba, 1-1-1 Tennodai, Ibaraki, Japan

2. International Center for Materials Nanoarchitectonics, National Institute for Materials Science, 1-1 Namiki, Ibaraki, Japan

3. Degree Programs in Life and Earth Sciences, University of Tsukuba, 1-1-1 Tennodai, Ibaraki, Japan

4. School of Chemical Sciences and Engineering, Hokkaido University, 13 Kita, 8 Nishi, Kita-ku, Sapporo, Hokkaido 060-8628, Japan

5. Microbiology Research Center for Sustainability, University of Tsukuba, 1-1-1 Tennodai, Ibaraki, Japan

[#]**Corresponding author**:

Y. T.: tokunou.yoshihide.ga@u.tsukuba.ac.jp

KEYWORDS: Bacterial communities, Multicellular assemblages, Extracellular electron transfer, *C*-type cytochromes, Bacterial colony, *Bacillus subtilis*

Abstract

The metabolic activity of microorganisms in multicellular assemblages is limited by structural constraints and resource availability. To overcome these limitations, some bacteria utilize electron conduction in their communities to drive their metabolism, which has led to the development of various biotechnologies, such as electrochemical microbial systems and anaerobic digestion. However, measuring the conductivity among bacterial cells is difficult when they scarcely form stable biofilms on electrodes, which renders it difficult to identify the biomolecules involved in electron conduction. In the present study, we aimed to identify the proteins involved in electron conduction in *Shewanella oneidensis* MR-1 and examine the molecular mechanisms. We established a colony-based current–voltage measurement system that quantifies bacterial electrical conductivity, without the need for biofilm formation on electrodes. This assay enabled the quantification of the conductivity of gene deletion mutants that scarcely form biofilms on electrodes, demonstrating that *c*-type cytochromes, MtrC and OmcA, are involved in electron conduction. Furthermore, the use of colonies of gene deletion mutants demonstrated that flavins participate in electron conduction by binding to cytochromes on their outer membrane, providing insight into the electron conduction pathways at the molecular level. Furthermore, the conductivity of *Bacillus subtilis* 3610 colonies was determined to be approximately 23 times lower than that of MR-1 colonies, indicating that this approach can be used for various bacteria, including weak electricigens. The present assay provides a platform for rapidly identifying conductive bacterial colonies and components, linking bacterial energy conservation with electron transfer in multicellular communities.

1. Introduction

Bacteria form multicellular assemblages, such as colonies, biofilms, and flocks, and communicate with each other [1-4]. Such multicellular communities comprise the majority of bacteria in most natural and pathogenic ecosystems [1-4]. Multicellular architectures are enclosed by a matrix of extracellular polymeric substances with a thickness of several tens or hundreds of micrometers, creating a chemical gradient of biological resources that constrains metabolic activity and their development [5-6]. Dealing with resource gradients and limitations is a fundamental challenge for bacteria to thrive in multicellular form. Understanding the mechanisms underlying resource gradients would contribute to the control of multicellular bacterial communities.

Recent studies have proposed that bacteria in biofilms and colonies electrically overcome the shortage of biological resources required for their growth. The development of cell aggregates is often suppressed by the limitation of electron acceptors for bacteria (oxidants such as oxygen, nitrate, carbon dioxide, and fumarate), which are required for terminating respiratory processes and photosynthetic reactions to generate ATP [7]. Bacteria in an oxidant-limited zone can conserve energy by channeling intracellular electrons toward an oxidant-rich zone over cellular length [8]. Energy conservation sustained by electron transfer in bacterial communities is observed in diverse environments with significant implications for various phenomena and technologies, such as biogeochemical cycling [3], microbial electrochemical systems [9], anaerobic digestion [10], and pathogen treatment [8]. For example, the biofilm growth of *Geobacter sulfurreducens* on electrodes and minerals is supported by electron transfer over several tens of micrometers [11-12]. In another example, electrical conductivity of methane-oxidizing consortia within methane-seep sediments creates the syntropy of anaerobic methanotrophic archaea and sulfate-reducing bacteria [13-14]. Additionally, electron transfer in a biofilm of *Pseudomonas aeruginosa*, a pathogen causing cystic fibrosis, enables energy conservation in oxygen-limited zones, enhancing antibiotic resistance [15-16]. The electron transfer in aggregates is composed of two processes; 1. exporting electrons extracellularly across the bacterial membrane via membrane proteins, nanowires, and/or soluble redox molecules, through a process termed extracellular electron transfer (EET), and 2. conducting electrons over cellular length along the matrix in a community or cellular surfaces [8]. Although EET mechanisms have been extensively studied [17], the methodology for measuring the conductivity among bacterial cells is strictly limited; thus, the biomolecules involved in electron conduction and approaches for enhancing conductivity have been scarcely identified.

The conductivity of bacterial aggregation has been electrochemically measured using biofilms formed on electrodes [18-19] including interdigitated microelectrode arrays (IDA), where two interdigitated electrodes face each other at a distance of several micrometers [20]; thus, conductivity measurements have been limited to bacteria that stably form biofilms such as *Geobacter* [21]. Most bacteria including those with low EET capability (weak electricigens) distributed in natural environments scarcely form stable biofilms on electrodes [22-23] and thus, even the insight into the electron conduction mechanisms of a model EET-capable bacterium, *Shewanella*, is strictly limited. MR-1 possesses *c*-type cytochrome complexes (Cyts), such as the MtrCAB-OmcA complex, on its outer membrane and nanowire extensions, which act as EET pathways, however, the molecular mechanisms underlying the electron conduction through Cyts have merely been studied. MtrC and OmcA are *c*-type cytochromes located on the cell surface that receive electrons from the cytochrome-porin complex buried in the outer membrane, MtrAB, delivering electrons to the electrodes [24-25]. MR-1 secretes flavins extracellularly, which mediate EET from MtrC/OmcA to electrodes, acting as bound redox cofactors of MtrC/OmcA and electron shuttles diffusing between MtrC/OmcA and the electrodes [26-28]. Since MtrC and OmcA are exposed to the cell exterior, diffusing on the outer membrane [29], they have been proposed to participate in electron conduction over cellular length along the outer membrane [30]. Although involvement of Cyts in electron conduction has been suggested, according to the electrochemical measurement of MR-1 wild-type (WT) and the calculation of thermal activation energy [31], identification of electron conducting protein has been a challenge due to the difficulty in the use of gene deletion mutants for Cyts. Because gene deletion mutants scarcely grow and form biofilms on electrodes owing to the suppression of metabolism and weak EET capability [32], the conductivity of gene deletion mutants have not been quantified, rendering it difficult to identify the electron conducting proteins and clarify molecular mechanisms underlying the electron conduction.

In the present study, we quantified the electrical conductivity of gene deletion mutants for MtrC and OmcA of *Shewanella oneidensis* MR-1. We established a novel colony-based current–voltage measurement system that quantifies bacterial electrical conductivity, without the need for biofilm formation on IDA (Fig 1a), enabling conductivity quantification of gene deletion mutants. Furthermore, associated with bipotentiostat measurements, the colony-based measurement provided the insight into the molecular mechanisms underlying flavin-based electron conduction. The conductivity of a *Bacillus subtilis* 3610 colony was also quantified for evaluating the use of the present approach for colony-forming bacteria except for *S. oneidensis* MR-1.

2. Results and Discussion

2.1 Electrical conductivity measurement of *S. oneidensis* colonies

We first examined the electrical conductivity of *Shewanella oneidensis* MR-1 colonies. MR-1 cells were grown on LB agar by incubation for 24 h after spotting 10 μL of cell suspension at $OD_{600} = 0.25$, resulting in the formation of a colony with a diameter of approximately 8 mm (Fig 1a and Table S1). The colony on the agar was placed on an IDA to directly face the interdigitated electrodes (Fig 1a). To test the electrical conductivity of MR-1 colony, potential bias was applied between the interdigitated electrodes in the range of −0.5 V to 0.5 V and, simultaneously, the conduction current was measured. The current increased with increasing potential bias in the presence of the colony (Fig 1b). In contrast, the current scarcely increased when agar was placed on the IDA without colonies, demonstrating that the clear current–voltage (*I–V*) profile was derived from the MR-1 colony and the agar showed low electrical conductivity in this experimental setup, similarly with previous report that showed negligible current from agar [33]. However, not only the conduction current across the colony but also the catalytic current from intracellular metabolisms possibly impacts the *I–V* curve [34-35]. Because different potentials are applied to each interdigitated electrode in the presence of a bias voltage, the catalytic current may differ for each electrode, leading to a higher apparent current at higher bias voltage [34-35]. To minimize the catalytic current from metabolisms, the colony was exposed to an antibiotics inhibiting protein synthesis, erythromycin (EM), at 4 mg mL^{-1} for 1 h. We confirmed that more than 99 % of the cells stopped the growth and the catalytic current decreased over 95 % (Fig S1 and Table S2). Although the slope decreased approximately four times, the current increased upon the application of bias voltage after exposure to EM (Fig 1b), which strongly suggests that the *I–V* curve represents the electrical conductivity of the MR-1 colony. Furthermore, the *I–V* profile showed a sigmoidal signature with steady-state currents at high voltages, which is characteristic of electron conduction driven by electron hopping among redox centers [36-37] and is consistent with the present model for electron conduction in MR-1 cells and biofilms [29, 31].

Because the *I–V* slope close to 0 V represents the conductance in the electron hopping model [36-37], the electrical conductivity of the colony was calculated from the *I–V* slope at −50 mV to 50 mV, colony thickness, and IDA configuration. The thickness of the colony was measured using the z-stack mode of confocal reflection microscopy with a dry lens, which provided a three-dimensional structure of the colony (Figs. 1c and S2). The microscopic image around the edge of the colony showed that the colony presented a hemispherical shape and a thickness of 138 ± 8 μm (Table S1). Because this thickness is sufficiently larger than the space between the

interdigitated electrodes, the conductivity is estimated to be independent of the colony thickness, as reported previously [21]. Using equation 3 presented in Experimental Section, the conductivity of the EM-exposed colony was calculated to be 2.2 ± 0.34 nS cm^{-1} (Fig 1d).

To quantitatively evaluate the validity of the electrical conductivity of EM-exposed colonies, we measured the conductivity of the live colony in bipotentiostat mode, which has been used for quantifying the conductivity of *Geobacter* biofilms formed on IDA [12, 21]. To control the potential of each interdigitated electrode as the source and drain electrodes, the IDA was connected to a bipotentiostat. Cyclic voltammetry was conducted on each electrode with a 20 mV difference between the source and drain electrodes at a scan rate of 1 mV s^{-1}. Ag/AgCl (sat. KCl) electrode and platinum wire were inserted into the agar as the reference and counter electrodes, respectively (Fig 1e). The cyclic voltammograms showed a catalytic current in both the source and drain electrodes, which is consistent with previous reports on MR-1 cells attached to electrodes (Fig S3)[31]. To measure the conduction current from the source to the drain electrode, the background contribution of the catalytic current was eliminated by subtracting the source current from the drain current, consistent with the method used in previous studies [31, 38]. The subtracted current showed a broad peak ranging from -0.2 V to 0.2 V with a peak potential at approximately -0.16 V vs standard hydrogen electrode (SHE) (Fig 1e). Because the peak was observed in both the positive and negative scans, it was not due to the different number of redox centers on each interdigitated electrode but the conduction current from the source to the drain electrode, which is consistent with previous reports [21, 31]. The conductance can be calculated with Ohm's law using the gating offset (source voltage – drain voltage) and the peak current (corresponding to twice the conduction current) when the gating offset is sufficiently small (Fig S4) [31, 39]. Consequently, the conductivity of the live MR-1 colony was 3.3 ± 1.2 nS cm^{-1} (Fig 1d), which is close to that of the EM-exposed colony, as calculated from the *I–V* curve. The colonies treated with other antibiotics and biocide showed almost identical *I–V* slopes and conductivities as those treated with EM (chloramphenicol, 1.9 ± 0.29 nS cm^{-1}; isopropanol, 2.8 ± 1.0 nS cm^{-1}) (Fig 1d), further supporting that EM scarcely disturbs the conductivity across the colony. A previous study reported that a combination of a genetic engineering approach and light-patterning enables the formation of a biofilm of 10 μm thickness on IDAs, which exhibits a conductivity of 4.5 nS cm^{-1} [39]. The present colony-based assay reveals the conductivity of the MR-1 population at the same order of magnitude without biofilm formation; this value is close to that obtained from simulation data, 7 nS cm^{-1} [29] (Fig 1d). Because the expression of genes corresponding to Cyts is limited in aerobic cultivation [40], the slightly lower conductivity of the

aerobic colony compared with that obtained from the simulation data is consistent with the present electron conduction model in which Cyts are the major carriers of electrons.
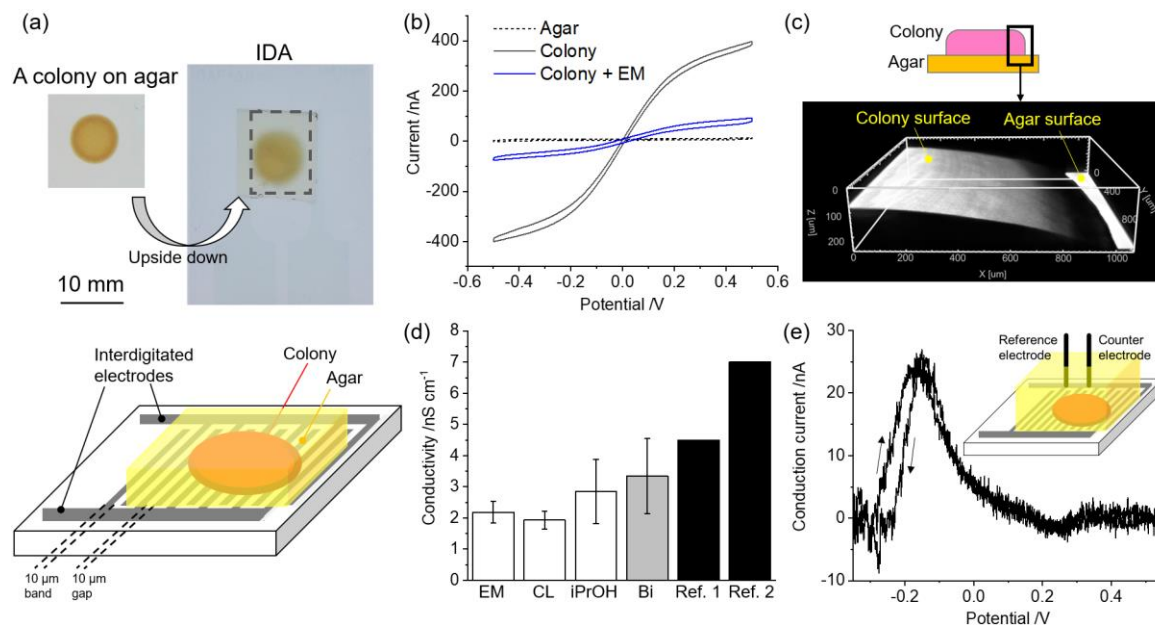

Figure 1. Electrical conduction measurement in *Shewanella oneidensis* MR-1 colonies. (a) A photograph of a *S. oneidensis* MR-1 colony on agar and on an interdigitated microelectrode array (IDA), and an illustration of a MR-1 colony on an IDA. Interdigitated electrodes (10 mm long and 10 μm wide) are patterned on the IDA with 10 μm wide gaps. (b) Representative current–voltage (*I–V*) profiles of MR-1 colonies before and after exposure to 4 mg mL^{-1} erythromycin (EM). The *I–V* curve of LB agar is depicted as a dashed line. (c) Three-dimensional image of a MR-1 colony observed with confocal reflection microscopy. (d) Electrical conductivity of MR-1 colonies. The conductivity estimated from the *I–V* profile is represented by white bars and that measured using a bipotentiostat (Bi) is shown by a gray bar. The colonies were treated with erythromycin 4 mg mL^{-1} (EM), chloramphenicol 20 mg mL^{-1} (CL), or isopropanol (iPrOH) as the biocide before the *I–V* measurement. Black bars represent the conductivities of MR-1 reported previously (Ref 1:[39] , Ref 2:[29]). Error bars represent the standard error of the mean (SEM) from at least three independent experiments. (e) Representative conduction current profile against the gate potential (the average of source and drain potential). The conductivity of the live colony was measured using a bipotentiostat with 20 mV difference between the source and drain electrodes at a scan rate of 1 mV s^{-1}; Ag/AgCl (sat. KCl) electrode and platinum wire were inserted into the agar as the reference and counter electrodes,

respectively. The arrows indicate the direction of potential sweep. Baseline was subtracted using a software, Qsoas [41].

2.2 Identification of proteins involved in electron conduction in *S. oneidensis* MR-1

To identify the proteins involved in the electron conduction, colonies of gene deletion mutants were subjected to the assay. We performed *I–V* measurement in a colony of a gene deletion mutant for *mtrC* (Δ*mtrC*). Although the growth of gene deletion mutants for Cyts decreased on the electrodes [32], the diameter and thickness of the Δ*mtrC* colony were almost identical to those of the WT (Fig S5 and Table S1). The *I–V* slope of this mutant (1.5 ± 0.25 nS cm-1) was lower than that of the WT (Fig 2a and c). This result demonstrates that the present assay can be applied to mutants for Cyts, which have been difficult to analyze using the conventional approach, and suggests that MtrC is involved in electron conduction in MR-1 cells. However, the extent of the decrease in electrical conductivity was limited to approximately 33%, suggesting that biomolecules other than MtrC are also involved in electrical conduction. We subsequently measured the conductivity of the gene deletion mutant for *omcA* (Δ*omcA*). The conductivity of the Δ*omcA* colony (1.4 ± 0.18 nS cm^{-1}) was lower than that of the WT (Fig 2b and c), suggesting that OmcA, as well as MtrC, conducts electrons in the colony. A mutant, named LS527, lacking all Cyts (*mtrCAB* (SO_1776-SO_1778), *mtrDEF* (SO_1780-SO_1782), and *omcA* (SO_1779)), showed further decrease in conductivity (0.49 ± 0.09 nS cm^{-1}; Fig 2b and c). These data demonstrate that Cyts including MtrC and OmcA primarily contribute to electron conduction in the colony.
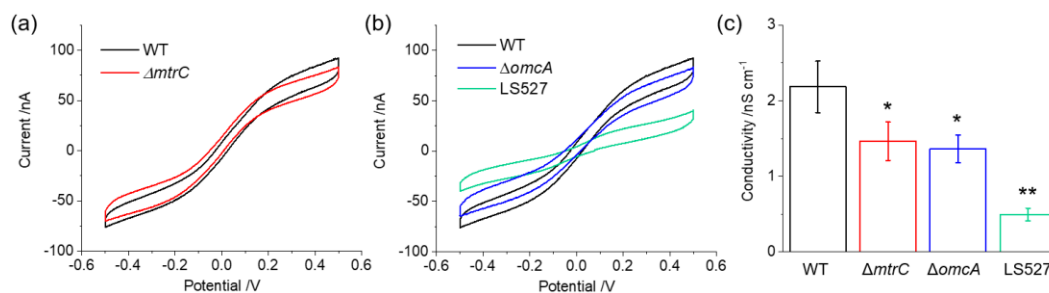

Figure 2. (a and b) Representative *I–V* profiles of *S. oneidensis* MR-1 mutants after exposure to 4 mg mL^{-1} EM. The data for WT is identical to the data in Figure 1b. (c) Electrical conductivity of MR-1 mutants. Error bars

represent the SEM from at least three independent experiments. Statistical significance is determined by *P*-values from unpaired one-tailed Student's *t* tests comparing to WT and are represented as follows: *$p < 0.05$ and **$p < 0.01$.

2.3 Involvement of flavin–Cyt complexes in electrical conduction in *S. oneidensis* MR-1

To examine the effect of flavins on electron conduction, we measured the conductivity of a gene deletion mutant for the flavin exporter *bfe* (Δ*bfe*) [42]. Although the shape of the colony of this mutant strain was similar to that of the WT (Fig S5), the *I–V* slope for this mutant was lower than that for the WT and the conductivity of Δ*bfe* was 1.2 ± 0.11 nS cm^{-1} (Figs 3a and c). These results demonstrate that extracellular flavins are involved in electron conduction in MR-1 cells. To further confirm the impact of flavins on electrical conductivity, we grew WT colonies on LB agar containing 10 μM flavin mononucleotides (FMN) (Fig S6). The colony showed a conductivity of 5.5 ± 0.83 nS cm^{-1}, which is approximately 2.5 times higher than that without FMN addition. Furthermore, the addition of FMN into agar complemented the conductivity of the Δ*bfe* colony (4.3 ± 0.48 nS cm^{-1}) to a similar extent as that for WT, suggesting that the decrease in Δ*bfe* conductivity without additional FMN was due to the loss of flavin in the colony. To minimize the interference of FMN in colony growth, we grew the WT colony on LB agar for 24 h and added 50 μL of 50 μM FMN 10 min before measurement. The slope of the *I–V* curve clearly increased under this condition (Fig S7), confirming that the increase in the *I–V* slope originates from the change in the electrical conductivity rather than colony growth.

To test the flavin–Cyt interaction during electron conduction, the conductivity of LS527 grown on FMN-containing LB agar was measured. The slope of the *I–V* curve was significantly lower than that for WT, with a conductivity of 1.4 ± 0.05 nS cm^{-1} (Fig 3b), indicating that Cyts contribute to electron conduction in the presence of FMN. To obtain molecular insights into the flavin–Cyt interaction, gating measurements were conducted on the Δ*bfe* colony using bipotentiostat and compared with the results for WT (Figs 3c and S3). Whereas the peak intensity was slightly different between forward and backward scan probably due to slight difference of the amounts of redox species on each interdigitated electrode, the conduction peak observed for the Δ*bfe* colony ranged from −0.2 V to 0.2 V, similar to that for WT (Fig 3c). However, the peak intensity at −0.16 V significantly decreased, suggesting that the conduction peak at −0.16 V corresponds to that of flavins in the WT colony. The peak potential of approximately −0.16 V is almost identical to the redox potential of flavins acting as bound redox cofactor in Cyts (−0.145 V vs SHE in ref. [27]). The peak corresponding to shuttling flavins was not detected (−0.26 V vs SHE in ref.

[27]) (Fig 3c). These data strongly suggest that flavins in the colony conduct electrons not as shuttling mediators but as bound redox cofactors in Cyts, in this experimental setup. The potential of the broad shoulder peak observed in both WT and Δ*bfe* was almost identical to that of multi-hemes in Cyts (typically ranging from −0.1 V to 0.2 V [27, 31]). Collectively, these results strongly suggest that the flavin–Cyt complex conducts electrons in the MR-1 colonies.

The present study provides insights regarding the flavin-binding site and electron conduction mechanisms. Because the 10 hemes of MtrC and OmcA are arranged in a "staggered-cross" configuration, hemes 2, 1, 6, and 7, which are laterally aligned against the outer membrane, are proposed to mediate electron transfer along the cell surface (Fig 3d) [29, 38, 43]. In contrast, the suggested binding site of flavins differs among studies [44-46], probably because of the high structural flexibility and binding affinity in response to surrounding conditions such as the redox state [47] and mechanical stress [38, 48]. This implies the importance of identifying the binding site during electron transfer. As the present study demonstrated that flavins bind to Cyts near the lateral electron transfer pathway, the binding site and electron conduction mechanisms can be speculated. Electronic structure calculations and molecular simulations indicated that the lateral electron transfer through hemes 2, 1, 6, and 7 was efficient, similar to the electron transfer pathway from the cell interior to the exterior (hemes 10 to 5) in MtrC [43]. Therefore, the electron transfer between adjacent Cyt complexes (MtrC/MtrC, MtrC/OmcA, OmcA/OmcA) can be considered to be enhanced by flavins, implying that the possible flavin-binding site is near the outer hemes 2 and/or 7 (Fig 3d). Although the kinetics of inter-Cyt electron transfer is unclear because of the lack of insight into the Cyts/Cyt docking structure, the outer hemes 2 and 7 are located at the side of the β-barrels in domains I and III [44]. Thus, the inter-heme distance between heme 7 and neighboring heme 2 in adjacent Cyts is possibly longer than the inter-heme distance in each cytochrome, and electron transfer could be accelerated by flavins shortening the electron transfer length (Fig 3d).
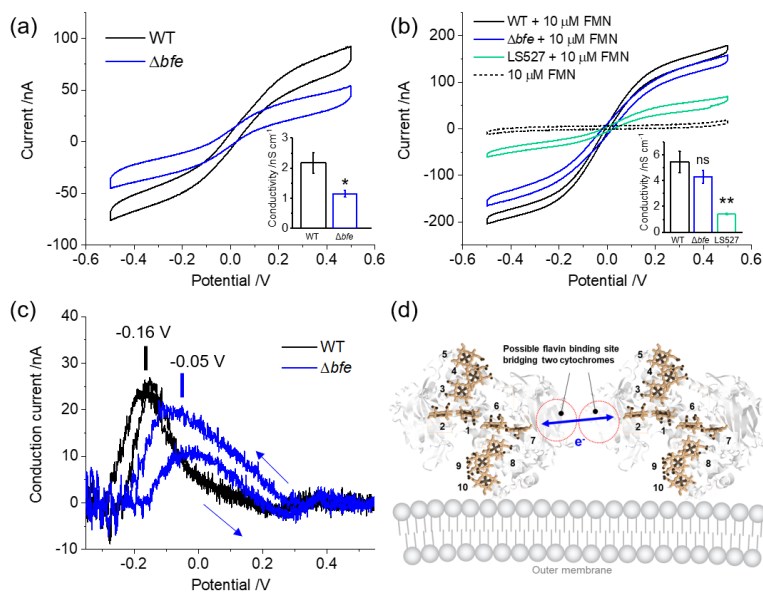
Figure 3. Representative *I–V* profiles of MR-1 WT and Δ*bfe* (a) and WT, Δ*bfe*, and LS527 in the presence of 10 µM FMN in agar (b) after exposure to 4 mg mL^{-1} EM. The data for WT (a) is identical to the data in Figure 1b. The dashed line represents the data of LB agar containing 10 µM FMN without colonies. Insets: The conductivity of each strain. Error bars represent the SEM from at least three independent experiments. Statistical significance is determined by *P*-values from unpaired one-tailed Student's *t* tests comparing to WT and are represented as follows: *p < 0.05, **p < 0.01, and ns (not significant) *p* > 0.05. (c) Representative conduction current profile of WT (black line) and Δ*bfe* (blue line) against the gate potential. The data for WT is identical to that in Figure 1e. Baseline was subtracted using the software Qsoas [41]. (d) A model of electron conduction in MR-1 colonies mediated by flavin-Cyts complexes. The deca-hemes in the crystal structure of the MtrC protein (PDB code: 4LM8) are highlighted, and a proposed flavin binding site is illustrated.

2.4 Electrical conduction in *B. subtilis* 3610 colonies

We applied this assay to *B. subtilis* 3610, which is a gram-positive bacterium that has been studied as a model system in microbiology, especially in studies related to biofilms and colonies [49]. Recent studies have evaluated the EET capability of *B. subtilis*, suggesting that electron conduction in biofilms supports energy conservation using matrix-associated extracellular irons [23]. However, the electrical conductivity of *B. subtilis* has not been quantified, because *B. subtilis* forms pellicle biofilms at the air/liquid interface rather than at the substrate surface [50]. Here, a

colony of *B. subtilis* 3610 was formed on LB agar, and conductivity was estimated using *I–V* measurements. Because of their slight resistance to EM and CL, the colonies were exposed to kanamycin (KM). The *I–V* slope of the *B. subtilis* colony was substantially larger than that of the LB agar (Fig 4a and S8), demonstrating electron conduction in the colony. Because the thickness of the colony was thinner than that of MR-1, comparable to the gap between interdigitated electrodes (15.7 ± 1.20 μm, Fig S9 and Table S1), the conductivity depends on the thickness, as reported previously [39, 51]. The conductivity was determined to be 0.094 ± 0.008 nS cm^{-1}, which is approximately 23 times lower than that of the MR-1 colony (Fig 4b). The conductivity increased to 0.32 ± 0.022 nS cm^{-1} upon addition of FMN in the agar (Figs 4 a and b). Because long-range electron transfer over several tens or hundreds of micrometers along nanowires drives the metabolism of MR-1 [52], even if the electrical conductivity of *B. subtilis* 3610 is one order of magnitude lower than that of MR-1, it may support electron transfer over several micrometers, which is longer than the cellular length, conserving energy production. Upon application of the potential bias, the current increase was almost linear rather than sigmoidal, similar to the charge transport along the DNA [53], strongly suggesting that this strain transports electrons via different mechanisms compared with MR-1. Identifying the electron carriers and unraveling the molecular mechanisms of long-range electron transfer would be of great interest. Considering that *B. subtilis* is a model industrial bacterium for flavin-production [54], self-produced flavins possibly act as electron carriers in *B. subtilis* biofilms in nature.
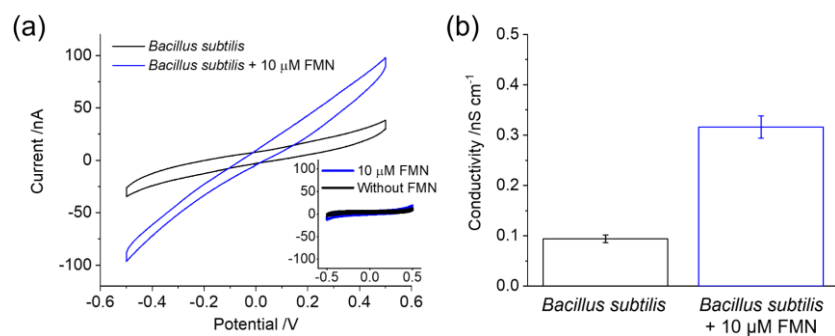

Figure 4. (a) Representative *I–V* profiles of *Bacillus subtilis* 3610 colonies on LB agar (black line) and LB agar containing 10 μM FMN after exposure to 10 mg mL^{-1} kanamycin (KM) for 2 h. Inset: Representative *I–V* profiles agar without colonies. (b) Electrical conductivity of *B. subtilis* 3610 colonies on LB agar (black bar) and LB agar containing 10 μM FMN (blue bar). Error bars represent the SEM from at least three independent experiments.

3. Conclusion

We developed a methodology to measure the electrical conductivity of bacterial multicellular assemblages based on I–V profiles of colonies placed on IDAs. Because the process of biofilm growth on electrodes can be avoided, the present assay can easily quantify the impact of gene deletion on conductivity. The I–V profiles revealed MtrC and OmcA are involved in electron conduction in *S. oneidensis* MR-1 colonies and that flavins form complexes with Cyts during electron conduction. These data enable speculation of the flavin–Cyt binding positions and electron conduction mechanisms, suggesting that flavin-Cyts complexes contributes to power output in microbial fuel cells by accelerating electron transfer among MR-1 cells as well as electron transfer at MR-1/electrode interface. Furthermore, the present assay quantified conductivity of *B. subtilis* colonies. Colonies are a major form of bacterial communities, and they have been used for growing and isolating bacteria in laboratories throughout the history of microbiology. Most culturable bacteria grow in the form of colonies; thus, colony-based assays are expected to be applicable to versatile bacteria, regardless of their ability to form biofilms on electrode surfaces. Considering that I–V profiles can be obtained in high-throughput systems, the present assay provides a platform for rapidly identifying conductive bacterial colonies and conductive components, enabling the development of biotechnologies such as high-performance microbial electrochemical systems, anaerobic digestion, and the control of pathogenic biofilms.

Supporting Information**. Experimental procedures, confocal reflection microscopic images, current-voltage profiles.**

Corresponding Authors

* Y. T.: tokunou.yoshihide.ga@u.tsukuba.ac.jp

N. N.: nomura.nobuhiko.ge@u.tsukuba.ac.jp

Author Contributions

All authors wrote the manuscript and discussed the results. All authors have given approval to the final version of the manuscript.

Declaration of competing interest

The authors declare no known competing financial interests.

REFERENCES

1.   Costerton, J. W.; Stewart, P. S.; Greenberg, E. P., Bacterial biofilms: A common cause of persistent infections. *Science* **1999,** *284* (5418), 1318-1322.

2.   Camara, M.; Green, W.; MacPhee, C. E.; Rakowska, P. D.; Raval, R.; Richardson, M. C.; Slater-Jefferies, J.; Steventon, K.; Webb, J. S., Economic significance of biofilms: a multidisciplinary and cross-sectoral challenge. *NPJ Biofilms Microbiomes* **2022,** *8* (1), 42.

3.   Sentenac, H.; Loyau, A.; Leflaive, J.; Schmeller, D. S., The significance of biofilms to human, animal, plant and ecosystem health. *Funct. Ecol.* **2022,** *36* (2), 294-313.

4.   Bui, B. T. S.; Auroy, T.; Haupt, K., Fighting Antibiotic-Resistant Bacteria: Promising Strategies Orchestrated by Molecularly Imprinted Polymers. *Angew. Chem. Int. Ed.* **2022,** *61* (8), e202106493.

5.   Kim, J.; Hahn, J. S.; Franklin, M. J.; Stewart, P. S.; Yoon, J., Tolerance of dormant and active cells in *Pseudomonas aeruginosa* PA01 biofilm to antimicrobial agents. *J. Antimicrob. Chemoth.* **2009,** *63* (1), 129-135.

6.   Jo, J. Y.; Price-Whelan, A.; Dietrich, L. E. P., Gradients and consequences of heterogeneity in biofilms. *Nat. Rev. Microbiol.* **2022,** *20*, 593-607.

7.   Saunders, S. H.; Tse, E. C. M.; Yates, M. D.; Otero, F. J.; Trammell, S. A.; Stemp, E. D. A.; Barton, J. K.; Tender, L. M.; Newman, D. K., Extracellular DNA Promotes Efficient Extracellular Electron Transfer by Pyocyanin in *Pseudomonas aeruginosa* Biofilms. *Cell* **2020,** *182* (4), 919-932.

8.   Tokunou, Y.; Toyofuku, M.; Nomura, N., Physiological Benefits of Oxygen-Terminating Extracellular Electron Transfer. *Mbio* **2022,** *13* (6), e01957-22.

9.   Malvankar, N. S.; Tuominen, M. T.; Lovley, D. R., Biofilm conductivity is a decisive variable for high-current-density Geobacter sulfurreducens microbial fuel cells. *Energy Environ. Sci.* **2012,** *5* (2), 5790-5797.

10.   Nabi, M.; Liang, H.; Cheng, L.; Yang, W. B.; Gao, D. W., A comprehensive review on the use of conductive materials to improve anaerobic digestion: Focusing on landfill leachate treatment. *J. Environ. Manage.* **2022,** *309*, 114540.

11.   Malvankar, N. S.; Vargas, M.; Nevin, K. P.; Franks, A. E.; Leang, C.; Kim, B. C.; Inoue, K.; Mester, T.; Covalla, S. F.; Johnson, J. P.; Rotello, V. M.; Tuominen, M. T.; Lovley, D. R., Tunable metallic-like conductivity in microbial nanowire networks. *Nat. Nanotechnol.* **2011,** *6* (9), 573-579.

12.   Yates, M. D.; Strycharz-Glaven, S. M.; Golden, J. P.; Roy, J.; Tsoi, S.; Erickson, J. S.; El-Naggar, M. Y.; Barton, S. C.; Tender, L. M., Measuring conductivity of living *Geobacter sulfurreducens* biofilms. *Nat. Nanotechnol.* **2016,** *11* (11), 910-913.

13.   McGlynn, S. E.; Chadwick, G. L.; Kempes, C. P.; Orphan, V. J., Single cell activity reveals direct electron transfer in methanotrophic consortia. *Nature* **2015,** *526* (7574), 531-535.

14.   Wegener, G.; Krukenberg, V.; Riedel, D.; Tegetmeyer, H. E.; Boetius, A., Intercellular wiring enables electron transfer between methanotrophic archaea and bacteria. *Nature* **2015,** *526* (7574), 587-590.

15.   Dietrich, L. E. P.; Okegbe, C.; Price-Whelan, A.; Sakhtah, H.; Hunter, R. C.; Newman, D. K., Bacterial Community Morphogenesis Is Intimately Linked to the Intracellular Redox State. *J. Bacteriol.* **2013,** *195* (7), 1371-1380.

16.   Schiessl, K. T.; Hu, F. H.; Jo, J.; Nazia, S. Z.; Wang, B.; Price-Whelan, A.; Min, W.; Dietrich, L. E. P., Phenazine production promotes antibiotic tolerance and metabolic heterogeneity in *Pseudomonas aeruginosa* biofilms. *Nat. Commun.* **2019,** *10*, 762.

17.   Shi, L.; Dong, H. L.; Reguera, G.; Beyenal, H.; Lu, A. H.; Liu, J.; Yu, H. Q.; Fredrickson, J. K., Extracellular electron transfer mechanisms between microorganisms and minerals. *Nat. Rev. Microbiol.* **2016,** *14* (10), 651-662.

18.   Okamoto, A.; Hashimoto, K.; Nakamura, R., Long-range electron conduction of *Shewanella* biofilms mediated by outer membrane *C*-type cytochromes. *Bioelectrochemistry* **2012,** *85*, 61-65.

19.   Zhang, X.; Philips, J.; Roume, H.; Guo, K.; Rabaey, K.; Prevoteau, A., Rapid and Quantitative Assessment of Redox Conduction Across Electroactive Biofilms by using Double Potential Step Chronoamperometry. *Chemelectrochem* **2017,** *4* (5), 1026-1036.

20.   Malvankar, N. S.; Lovley, D. R., Electronic Conductivity in Living Biofilms: Physical Meaning, Mechanisms, and Measurement Methods. *Biofilms in Bioelectrochemical Systems: From Laboratory Practice to Data Interpretation* **2015**, 211-247.

21.   Yates, M. D.; Golden, J. P.; Roy, J.; Strycharz-Glaven, S. M.; Tsoi, S.; Erickson, J. S.; El-Naggar, M. Y.; Barton, S. C.; Tender, L. M., Thermally activated long range electron transport in living biofilms. *Phys. Chem. Chem. Phys.* **2015,** *17* (48), 32564-32570.

22.   Doyle, L. E.; Marsili, E., Weak electricigens: A new avenue for bioelectrochemical research. *Bioresour. Technol.* **2018,** *258*, 354-364.

23.   Qin, Y. X.; He, Y. H.; She, Q. X.; Larese-Casanova, P.; Li, P. L.; Chai, Y. R., Heterogeneity in respiratory electron transfer and adaptive iron utilization in a bacterial biofilm. *Nat. Commun.* **2019,** *10*.

24.   Hartshorne, R. S.; Reardon, C. L.; Ross, D.; Nuester, J.; Clarke, T. A.; Gates, A. J.; Mills, P. C.; Fredrickson, J. K.; Zachara, J. M.; Shi, L.; Beliaev, A. S.; Marshall, M. J.; Tien, M.; Brantley, S.; Butt, J. N.; Richardson, D. J., Characterization of an electron conduit between bacteria and the extracellular environment. *Proc. Natl. Acad. Sci. U. S. A.* **2009,** *106* (52), 22169-22174.

25.   Edwards, M. J.; White, G. F.; Butt, J. N.; Richardson, D. J.; Clarke, T. A., The Crystal Structure of a Biological Insulated Transmembrane Molecular Wire. *Cell* **2020,** *181* (3), 665-673.

26.   Marsili, E.; Baron, D. B.; Shikhare, I. D.; Coursolle, D.; Gralnick, J. A.; Bond, D. R., Shewanella Secretes flavins that mediate extracellular electron transfer. *Proc. Natl. Acad. Sci. U. S. A.* **2008,** *105* (10), 3968-3973.

27.   Okamoto, A.; Hashimoto, K.; Nealson, K. H.; Nakamura, R., Rate enhancement of bacterial extracellular electron transport involves bound flavin semiquinones. *Proc. Natl. Acad. Sci. U. S. A.* **2013,** *110* (19), 7856-7861.

28.   Xu, S.; Jangir, Y.; El-Naggar, M. Y., Disentangling the roles of free and cytochrome-bound flavins in extracellular electron transport from *Shewanella oneidensis* MR-1. *Electrochim. Acta* **2016,** *198*, 49-55.

29.   Chong, G. W.; Pirbadian, S.; Zhao, Y.; Zacharoff, L. A.; Pinaud, F.; El-Naggar, M. Y., Single molecule tracking of bacterial cell surface cytochromes reveals dynamics that impact long-distance electron transport. *Proc. Natl. Acad. Sci. U. S. A.* **2022,** *119* (19), e2119964119.

30.   Okamoto, A.; Nakamura, R.; Hashimoto, K., In-vivo identification of direct electron transfer from *Shewanella oneidensis* MR-1 to electrodes via outer-membrane OmcA-MtrCAB protein complexes. *Electrochim. Acta* **2011,** *56* (16), 5526-5531.

31.   Xu, S.; Barrozo, A.; Tender, L. M.; Krylov, A. I.; El-Naggar, M. Y., Multiheme Cytochrome Mediated Redox Conduction through *Shewanella oneidensis* MR-1 Cells. *J. Am. Chem. Soc.* **2018,** *140* (32), 10085-10089.

32.   Bretschger, O.; Obraztsova, A.; Sturm, C. A.; Chang, I. S.; Gorby, Y. A.; Reed, S. B.; Culley, D. E.; Reardon, C. L.; Barua, S.; Romine, M. F.; Zhou, J.; Beliaev, A. S.; Bouhenni, R.; Saffarini, D.; Mansfeld, F.; Kim, B. H.; Fredrickson, J. K.; Nealson, K. H., Current production and metal oxide reduction by *Shewanella oneidensis* MR-1 wild type and mutants. *Appl. Environ. Microb.* **2007,** *73* (21), 7003-7012.

33.   Long, X. Z.; Li, W. P.; Okamoto, A., Riboflavin-rich agar enhances the rate of extracellular electron transfer from electrogenic bacteria inside a thin-layer system. *Bioelectrochemistry* **2022,** *148*, 108252.

34.   Ding, M. N.; Shiu, H. Y.; Li, S. L.; Lee, C. K.; Wang, G. M.; Wu, H.; Weiss, N. O.; Young, T. D.; Weiss, P. S.; Wong, G. C. L.; Nealson, K. H.; Huang, Y.; Duan, X. F., Nanoelectronic Investigation Reveals the Electrochemical Basis of Electrical Conductivity in *Shewanella* and *Geobacter*. *ACS Nano* **2016,** *10* (11), 9919-9926.

35.   Liu, P. P.; Liang, P.; Beyenal, H.; Huang, X., Overestimation of biofilm conductance determined by using the split electrode as the microbial respiration. *J. Power Sources* **2020,** *453*.

36.   Dalton, E. F.; Surridge, N. A.; Jernigan, J. C.; Wilbourn, K. O.; Facci, J. S.; Murray, R. W., Charge Transport in Electroactive Polymers Consisting of Fixed Molecular Redox Sites. *Chem. Phys.* **1990,** *141* (1), 143-157.

37.   Strycharz-Glaven, S. M.; Snider, R. M.; Guiseppi-Elie, A.; Tender, L. M., On the electrical conductivity of microbial nanowires and biofilms. *Energy Environ. Sci.* **2011,** *4* (11), 4366-4379.

38.   Long, X. Z.; Tokunou, Y.; Okamoto, A., Mechano-control of Extracellular Electron Transport Rate via Modification of Inter-heme Coupling in Bacterial Surface Cytochrome. *Environ. Sci. Technol.* **2023,** *57* (19), 7421–7430

39.   Zhao, F. J.; Chavez, M. S.; Naughton, K. L.; Niman, C. M.; Atkinson, J. T.; Gralnick, J. A.; El-Naggar, M. Y.; Boedicker, J. Q., Light-Induced Patterning of Electroactive Bacterial Biofilms. *ACS Synth. Biol.* **2022**.

40.   Myers, C. R.; Myers, J. M., Localization of Cytochromes to the Outer-Membrane of Anaerobically Grown *Shewanella-Putrefaciens* MR-1. *J. Bacteriol.* **1992,** *174* (11), 3429-3438.

41.   Fourmond, V., QSoas: A Versatile Software for Data Analysis. *Anal. Chem.* **2016,** *88* (10), 5050-2.

42.   Kotloski, N. J.; Gralnick, J. A., Flavin Electron Shuttles Dominate Extracellular Electron Transfer by *Shewanella oneidensis*. *mBio* **2013,** *4* (1), e00553-12.

43.   Jiang, X.; Burger, B.; Gajdos, F.; Bortolotti, C.; Futera, Z.; Breuer, M.; Blumberger, J., Kinetics of trifurcated electron flow in the decaheme bacterial proteins MtrC and MtrF. *Proc. Natl. Acad. U. S. A.* **2019**, *116* (9), 3425-3430.

44.   Edwards, M. J.; White, G. F.; Norman, M.; Tome-Fernandez, A.; Ainsworth, E.; Shi, L.; Fredrickson, J. K.; Zachara, J. M.; Butt, J. N.; Richardson, D. J.; Clarke, T. A., Redox Linked Flavin Sites in Extracellular Decaheme Proteins Involved in Microbe-Mineral Electron Transfer. *Sci. Rep.* **2015,** *5*, 11677.

45.   Paquete, C. M.; Fonseca, B. M.; Cruz, D. R.; Pereira, T. M.; Pacheco, I.; Soares, C. M.; Louro, R. O., Exploring the molecular mechanisms of electron shuttling across the microbe/metal space. *Front. Microbiol.* **2014,** *5*, 318.

46.   Babanova, S.; Matanovic, I.; Cornejo, J.; Bretschger, O.; Nealson, K.; Atanassov, P., Outer membrane cytochromes/flavin interactions in *Shewanella* spp.-A molecular perspective. *Biointerphases* **2017,** *12* (2), 021004.

47.   Tokunou, Y.; Chinotaikul, P.; Hattori, S.; Clarke, T. A.; Shi, L.; Hashimoto, K.; Ishii, K.; Okamoto, A., Whole-cell circular dichroism difference spectroscopy reveals an *in vivo*-specific deca-heme conformation in bacterial surface cytochromes. *Chem. Commun.* **2018,** *54* (99), 13933-13936.

48.   Tokunou, Y.; Okamoto, A., Geometrical Changes in the Hemes of Bacterial Surface *c*-Type Cytochromes Reveal Flexibility in Their Binding Affinity with Minerals. *Langmuir* **2019,** *35* (23), 7529-7537.

49.   Arnaouteli, S.; Bamford, N. C.; Stanley-Wall, N. R.; Kovacs, A. T., *Bacillus subtilis* biofilm formation and social interactions. *Nat. Rev. Microbiol.* **2021,** *19* (9), 600-614.

50.   Branda, S. S.; Gonzalez-Pastor, J. E.; Ben-Yehuda, S.; Losick, R.; Kolter, R., Fruiting body formation by Bacillus subtilis. *Proc. Natl. Acad. Sci. U. S. A.* **2001,** *98* (20), 11621-11626.

51.   Kankare, J.; Kupila, E. L., Insitu Conductance Measurement during Electropolymerization. *J. Electroanal. Chem.* **1992,** *322* (1-2), 167-181.

52.   Pirbadian, S.; Barchinger, S. E.; Leung, K. M.; Byun, H. S.; Jangir, Y.; Bouhenni, R. A.; Reed, S. B.; Romine, M. F.; Saffarini, D. A.; Shi, L.; Gorby, Y. A.; Golbeck, J. H.; El-Naggar, M. Y., *Shewanella oneidensis* MR-1 nanowires are outer membrane and periplasmic extensions of the extracellular electron transport components. *Proc. Natl. Acad. Sci. U. S. A.* **2014,** *111* (35), 12883-12888.

53.   Jimenez-Monroy, K. L.; Renaud, N.; Drijkoningen, J.; Cortens, D.; Schouteden, K.; van Haesendonck, C.; Guedens, W. J.; Manca, J. V.; Siebbeles, L. D. A.; Grozema, F. C.; Wagner, P. H., High Electronic Conductance through Double-Helix DNA Molecules with Fullerene Anchoring Groups. *J. Phys. Chem. A* **2017,** *121* (6), 1182-1188.

54.   Averianova, L. A.; Balabanova, L. A.; Son, O. M.; Podvolotskaya, A. B.; Tekutyeva, L. A., Production of Vitamin B2 (Riboflavin) by Microorganisms: An Overview. *Front. Bioeng. Biotech.* **2020,** *8*, 570828.